

Electronic transport in the Coulomb phase of the pyrochlore spin ice

Gia-Wei Chern,^{1,2} Saurabh Maiti,² Rafael M. Fernandes,³ and Peter Wölfle⁴

¹*Theoretical Division, T-4 and CNLS, Los Alamos National Laboratory, Los Alamos, NM, 87545, USA*

²*Department of Physics, University of Wisconsin, Madison, Wisconsin 53706, USA*

³*School of Physics and Astronomy, University of Minnesota, Minneapolis, MN 55455, USA*

⁴*Institute for Condensed Matter Theory and Institute for Nanotechnology,*

Karlsruhe Institute of Technology, D-76128 Karlsruhe, Germany

(Dated: July 4, 2018)

We investigate the transport properties of itinerant electrons interacting with a background of localized spins in a correlated paramagnetic phase of the pyrochlore lattice. We find a residual resistivity at zero temperature due to the scattering of electrons by the static dipolar spin-spin correlation that characterizes the metallic Coulomb phase. As temperature increases, thermally excited topological defects, also known as magnetic monopoles, reduce the spin correlation, hence suppressing electron scattering. Combined with the usual scattering processes in metals at higher temperatures, this mechanism yields a non-monotonic resistivity, displaying a minimum at temperature scales associated with the magnetic monopole excitation energy. Our calculations agree quantitatively with resistivity measurements in $\text{Nd}_2\text{Ir}_2\text{O}_7$, shedding light on the origin of the resistivity minimum observed in metallic spin-ice compounds.

The interaction between itinerant electrons and localized moments continues to attract considerable interest as model systems to understand non-Fermi liquid behaviors and unusual transport phenomena. Since the pioneering work of Kondo on the resistivity minimum in metals [1], the Kondo-lattice model has become the paradigm for a new class of problems [2]. This simple Hamiltonian describing the competition between Kondo screening of individual moments and direct exchange among localized spins plays an important role in the physics of heavy-fermion materials [3]. Novel magneto-transport phenomena such as colossal magnetoresistance [4] and anomalous Hall effect [5] emerge in a closely related double-exchange model in which the Kondo-screening is replaced by the effect of a ferromagnetic Hund's rule coupling [6].

Adding geometrical frustration to Kondo-lattice models opens a new avenue for exploring unconventional phase transitions and many-body states. For example, a spin-liquid phase with broken time-reversal symmetry and spontaneous Hall effect was recently observed in the pyrochlore iridate $\text{Pr}_2\text{Ir}_2\text{O}_7$ [7]. The conduction $5d$ electrons in this compound coexist with the localized $4f$ moments at the Pr sites that form a frustrated pyrochlore lattice (Fig. 1). A strong easy-axis anisotropy forces the moments to point along the local $\langle 111 \rangle$ directions. When spin interactions are restricted to nearest-neighbor ferromagnetic exchange J_F , an extensively large number of Ising configurations satisfying the “ice rules” are degenerate ground states [9]. As temperature tends to zero, this degeneracy is eventually lifted by residual perturbations, such as spin-electron coupling [10]. However, spatial spin correlations exhibit an unusual power-law decay over a wide temperature range below the Curie-Weiss constant $\Theta_{\text{CW}} \sim J_F/k_B$. Elementary excitations in this so-called Coulomb phase [11] are defect tetrahedra that violate the

ice rules and carry a finite magnetic charge [12, 13].

Recently, an unexpected resistivity minimum, similar to the one seen in Kondo systems, was observed in the paramagnetic phase of the metallic pyrochlore iridates $\text{Pr}_2\text{Ir}_2\text{O}_7$ and $\text{Nd}_2\text{Ir}_2\text{O}_7$ [14, 15]. Although quantum fluctuations of these Ising-like moments were shown to be non-negligible [16], the large easy-axis anisotropy suppresses the Kondo screening. On the other hand, a non-Kondo mechanism for the resistivity minimum was suggested by a recent numerical study of a strong-coupling Kondo-lattice model assuming classical Ising spins on the pyrochlore lattice [17]. In particular, their cellular dynamical mean-field calculation suggests a clear correlation between the position of resistivity minimum and the onset temperature of ice rules. However, up to date, there is not a transparent theory relating the resistivity of the Coulomb phase to its unique magnetic correlations and excitations.

In this paper, we present an analytical theory for electron transport in the Coulomb phase of spin ice. In the continuum approximation, the problem is recast into that of a correlated random “magnetic” field locally coupled to a Fermi sea of electrons. The resulting electronic scattering is the dominant transport mechanism at low temperatures. We show that thermally excited monopoles reduce the spin-spin correlation and suppress the electron scattering rate. Combined with the other scattering processes taking place in the metallic compounds - due, for instance, to electron-phonon interaction - we obtain a resistivity minimum at temperature scales associated with the excitation energy of the magnetic monopoles. We compare our calculations with the resistivity data on $\text{Nd}_2\text{Ir}_2\text{O}_7$ and find a good quantitative agreement. Our results show that strong geometrical frustration combined with topological excitations give rise to a resistivity minimum of non-Kondo character in metallic spin ice.

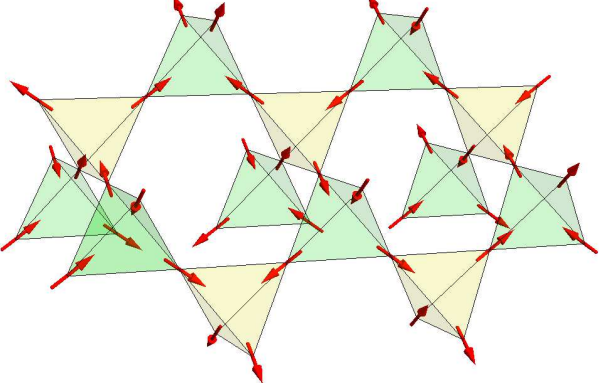


FIG. 1: (Color online) A fragment of the pyrochlore lattice. In the Coulomb phase, local spin arrangement on each individual tetrahedra obeys the so-called ice rules with two spins pointing in and two spins pointing out.

We start with a ferromagnetic Kondo-lattice model on the pyrochlore lattice:

$$\mathcal{H} = -t \sum_{\langle ij \rangle, \alpha} (c_{i, \alpha}^\dagger c_{j, \alpha} + \text{h.c.}) - J_H \sum_{i, \alpha \beta} \mathbf{S}_i \cdot \boldsymbol{\sigma}_{\alpha \beta} c_{i, \alpha}^\dagger c_{i, \beta} - J_F \sum_{\langle ij \rangle} \mathbf{S}_i \cdot \mathbf{S}_j. \quad (1)$$

Here the first term describes electron hopping between nearest-neighbor sites, t is the hopping integral, and $c_{i, \alpha}^\dagger$ creates an electron with spin $\alpha = \uparrow, \downarrow$ on site i . The itinerant electrons interact with the localized spins \mathbf{S}_i through an on-site Hund's coupling J_H ; here $\boldsymbol{\sigma}_{\alpha \beta}$ is a vector of Pauli matrices. As discussed above, the magnetic moments $\mathbf{S}_i = \tau_i S \hat{\mathbf{e}}_i$ are forced to point along the local $\hat{\mathbf{e}}_i = \langle 111 \rangle$ axes by a strong easy-axis anisotropy; $\tau_i = \pm 1$ is an Ising variable. The last term represents a ferromagnetic ($J_F > 0$) exchange interaction between neighboring moments.

We first consider the ground state of the localized spin system. The exchange energy of a single tetrahedron is minimized by six different Ising states with two spins pointing in and two pointing out of the tetrahedron. This 2-in-2-out rule is analogous to the Bernal-Fowler rule for water ice [9]. As explained by Pauling, the very large number of configurations satisfying the ice rule in a macroscopic sample gives rise to a measurable residual entropy at low temperatures [18]. Because of this huge degeneracy, spins remain disordered even at temperatures well below the exchange energy scale J_F .

Remarkably, spatial correlation of spins in this disordered yet highly constrained phase exhibits a power-law decay. This is because the local 2-in-2-out ice rule translates into a divergence-free condition $\nabla \cdot \mathbf{B} = 0$ for the coarse-grained magnetization field $\mathbf{B}(\mathbf{r}) = \sum_{i \in \mathcal{V}_r} \mathbf{S}_i / \Omega$, where \mathcal{V}_r denotes a coarse-graining block of volume

$\Omega \sim p_F^{-3}$ that contains several tetrahedra. In momentum space this constraint becomes $\mathbf{k} \cdot \mathbf{B}(\mathbf{k}) = 0$, indicating that only transverse fluctuations are allowed. Consequently, the static spin correlator has a dipolar form $\langle B_\mu(\mathbf{r}) B_\nu(0) \rangle \sim (\delta_{\mu\nu} - 3\hat{r}_\mu \hat{r}_\nu) / r^3$ for large r .

The low-energy excitations of this paramagnetic phase are topological defects that carry magnetic charges, namely, tetrahedra with 3-in-1-out or 1-in-3-out spin configurations. Since these emergent magnetic monopoles are sources and sinks for the magnetization field, hoppings of thermally excited monopoles modify the spin correlator at finite temperatures. In the low- T hydrodynamic regime, the relaxation of the magnetization by monopole motion is governed by a stochastic differential equation [12, 19]

$$\frac{\partial \mathbf{B}}{\partial t} = -2\mu n_m \Phi \mathbf{B} + D \nabla n_m + \boldsymbol{\zeta}(t), \quad (2)$$

Here $n_m = \nabla \cdot \mathbf{B}$ is the monopole density, μ and D are the monopole mobility and diffusion constant, respectively, $\boldsymbol{\zeta}(t)$ is a Gaussian noise source, $\Phi = (16/\sqrt{3}) a T$ indicates the entropic origin of monopole drift [12], and a is the lattice constant. The first term in the right-hand side of Eq. (2) implies a magnetic relaxation time $\tau_m \sim 1/\mu n_m \Phi$. Since the mobility $\mu \sim 1/T$ at low temperatures [19], the combination $\mu \Phi$ is a relatively weak function of T , and the relaxation time is governed by the monopole density: $n_m \sim e^{-\Delta/T}$ and diverges exponentially $\tau_m(T) = \tau_{m,0} e^{\Delta/T}$ [20]; here Δ is the activation energy for creating monopoles. Eq. (2) gives rise to a time-dependent correlation function [11, 21]:

$$\langle B_\mu(\mathbf{k}, t) B_\nu(-\mathbf{k}, 0) \rangle = \frac{1}{K} \left(\delta_{\mu\nu} - \frac{k_\mu k_\nu}{|\mathbf{k}|^2} \right) e^{-|t|/\tau_m} + \frac{1}{K} \frac{k_\mu k_\nu}{|\mathbf{k}|^2} \frac{\kappa^2}{(|\mathbf{k}|^2 + \kappa^2)} e^{-(1/\tau_m + D|\mathbf{k}|^2)|t|}, \quad (3)$$

where K is the stiffness constant of the flux field, $\kappa^{-1} = \ell_D \propto \sqrt{T/n_m}$ is the Debye screening length of monopoles. The two terms in Eq. (3) denote the transverse and longitudinal components, respectively.

Since the transport properties are dominated by conduction electrons near the Fermi surface, their wavefunction has a characteristic wave length p_F^{-1} which is much larger than the underlying lattice constant. Considering the low electron density of the iridate compounds, we can choose a coarse-graining block \mathcal{V} whose volume $\Omega \sim p_F^{-3}$. We thus consider a model Hamiltonian describing electrons interacting with the averaged magnetization field:

$$\mathcal{H} = \sum_{\mathbf{p}, \alpha} \varepsilon_{\mathbf{p}} c_{\mathbf{p}, \alpha}^\dagger c_{\mathbf{p}, \alpha} - \frac{g}{V} \sum_{\mathbf{p}, \mathbf{k}, \alpha \beta} \mathbf{B}(\mathbf{k}) \cdot \boldsymbol{\sigma}_{\alpha \beta} c_{\mathbf{p}, \alpha}^\dagger c_{\mathbf{p}+\mathbf{k}, \beta}, \quad (4)$$

where $\varepsilon_{\mathbf{p}}$ is the electron energy measured with respect to the chemical potential μ , $g \propto J_H$ is the coupling constant, and the correlation for the magnetization field

is given by Eq. (3). For simplicity, here we consider a parabolic dispersion $\varepsilon_{\mathbf{p}} = p^2/2m - \mu$, where m is the effective electron mass. Note that the Hamiltonian is weakly time-dependent owing to the slowly varying magnetic field. We first calculate the lifetime of electrons close to the Fermi surface. To this end, we consider the leading second-order terms of the electronic self-energy corresponding to the diagram shown in Fig. 2. Here the solid line denotes the free electron propagator $G_0(\mathbf{p}, \omega) = (\omega - \varepsilon_{\mathbf{p}} \pm i0)^{-1}$ with \pm sign corresponding to advanced/retarded Green's function, respectively, and the wavy line represents the \mathbf{B} -field correlator. Separating the correlator into the transverse and longitudinal components, we obtain a self-energy $\Sigma_{a,\alpha\beta} = \delta_{\alpha\beta} \Sigma_a$ whose imaginary part is given by

$$\text{Im}\Sigma_a(\mathbf{p}, \omega) = \frac{g^2}{2\pi^2 v K} \sum_{s=\pm 1} \int_0^\Lambda dk k \mathcal{D}_a(k) \times \tan^{-1} \left\{ \tau_a [vk - s(\omega - \varepsilon_p - k^2/2m)] \right\}, \quad (5)$$

Here $a = T, L$ labels the transverse and longitudinal components of the correlator, $v = p/m$ is the electron velocity, $\Lambda = \ell_c^{-1}$ is an ultraviolet cutoff, $\mathcal{D}_T = 2$ and $\mathcal{D}_L = \kappa^2/(k^2 + \kappa^2)$. The magnetic relaxation times are $\tau_T = \tau_m$ and $\tau_L = 1/(\tau_m^{-1} + D|\mathbf{k}|^2)$. Since the correlation (3) is valid only for coarse-grained magnetizations, the length scale ℓ_c should be over several lattice constants. A natural choice for the cutoff is the Fermi wavevector p_F . We note that our results do not depend on the exact value of the cutoff, as we show below.

We now consider the decay rate $\tau_e^{-1} = 2 \text{Im}\Sigma$ of electrons on the Fermi surface $\omega = \varepsilon_p = 0$. Fig. 3 shows the transverse and longitudinal components of $\text{Im}\Sigma$ as a function of temperature. In particular, the integral (5) for the transverse part depends only on two dimensionless parameters Λ/p_F and $\varepsilon_F \tau_{m,0}$, where ε_F is the Fermi energy. The longitudinal part, on the other hand, depends also on the monopole screening length ℓ_D . However, since at low temperature $\ell_D \gg \ell_c$ and $\mathcal{D}_L \ll \mathcal{D}_T$ for most of the integration region, the longitudinal contribution to the decay rate $\text{Im}\Sigma$ is negligible compared with the transverse part.

Interestingly, the transverse part $\text{Im}\Sigma_T$ decreases with increasing T . This is in stark contrast to the behavior of the scattering rate due to other common processes in metals, such as scattering by phonons, electrons, or spin fluctuations. The anomalous temperature dependence of

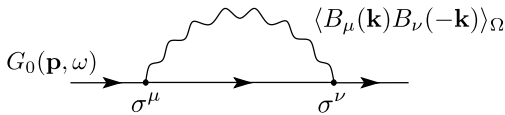


FIG. 2: Lowest-order diagram of the electron self-energy $\Sigma_{\alpha\beta}(\mathbf{p}, \omega)$. The solid and wavy lines denote the electron propagator G_0 and the spin correlator (3), respectively.

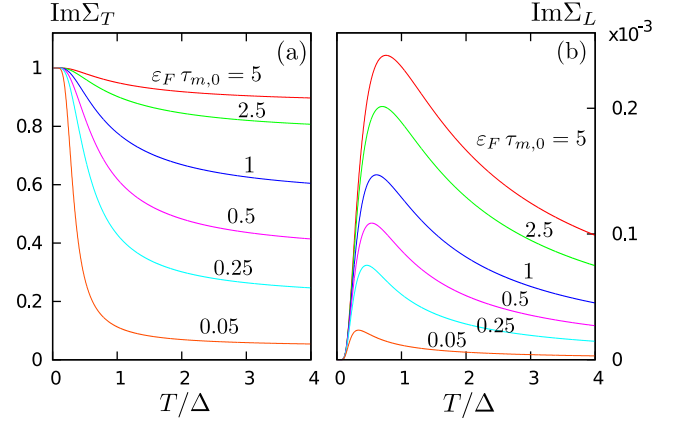


FIG. 3: (Color online) (a) Transverse and (b) longitudinal components of the electron scattering rate $\tau_e^{-1}(T) = 2 \text{Im}\Sigma$ as a function of temperature. Both are normalized with respect to $\text{Im}\Sigma_T(T=0) = g^2 \Lambda^2 / 2\pi v_F K$. We have used $\tau_{m,0} D p_F^2 = 0.1$ and a Debye screening length $\ell_D(T = \Delta) = 1.65 \times 10^3 \ell_c$ in the calculations.

$\text{Im}\Sigma$ can be understood as follows. At $T = 0$, a constant relaxation time results from scattering of electrons by a dipolar-correlated static random field. At finite temperatures, thermally excited monopoles reduce the spatial spin correlation and suppress the electron scattering rate. In particular, expanding $\text{Im}\Sigma_T(\mathbf{p}_F, \omega = 0)$ at low temperatures gives

$$\text{Im}\Sigma_T = \frac{g^2 \Lambda^2}{2\pi v_F K} \left(1 - \frac{4p_F^2}{\pi \Lambda^2} \frac{e^{-\Delta/T}}{\varepsilon_F \tau_{m,0}} \tanh^{-1} \frac{\Lambda}{2p_F} + \dots \right), \quad (6)$$

that decreases exponentially at small T . It should also be noted that at high temperatures $T \gg \Delta$, the correlator (3) of the coarse-grained magnetization is no longer valid due to proliferation of monopoles. Instead, a power-law relaxation rate $\tau_e^{-1} \propto T^n$ results from electron-phonon or electron-magnon scatterings. The competition of these two scattering mechanisms thus gives rise to a resistivity minimum.

We now turn to the calculation of the resistivity in the Coulomb phase, using the so-called memory function approach [22]. In this method the conductivity is expressed as $\sigma(z, T) = (i\omega_p^2/4\pi)[z + M(z, T)]^{-1}$, where $\omega_p^2 = 4\pi e^2 n_e/m$ is the electronic plasma frequency, n_e and m are the electron density and mass, respectively, and the *memory function* is approximated as $M(z) = (m/n_e z) [\phi(z) - \phi(0)]$ with

$$\phi(z) = -i \int_0^\infty dt e^{izt} \langle [[\mathcal{H}, j]_t, [\mathcal{H}, j]_{t=0}] \rangle. \quad (7)$$

Here $j = j_\mu = \sum_{\mathbf{p}} v_\mu(\mathbf{p}) c_{\mathbf{p},\alpha}^\dagger c_{\mathbf{p},\alpha}$ is the current operator ($\mu = x, y, z$), $v_\mu(\mathbf{p}) = \partial \varepsilon_{\mathbf{p}} / \partial p_\mu = p_\mu/m$, the Hamiltonian \mathcal{H} is given by Eq. (4), and $\langle \dots \rangle$ denotes average over the electronic ground state and degenerate spin configurations with correlations specified by Eq. (3).

Since, as discussed above, the scattering is dominated by the transverse part of the spin correlation, we thus focus on its contribution to the conductivity in the following discussion. A straightforward calculation gives

$$M(z) = \frac{4g^2}{3mn_e K} \int \frac{d^3\mathbf{p}}{(2\pi)^3} \frac{d^3\mathbf{k}}{(2\pi)^3} |\mathbf{k}|^2 \quad (8)$$

$$\times \frac{f(\varepsilon_{\mathbf{p}+\mathbf{k}}) - f(\varepsilon_{\mathbf{p}})}{(z + \varepsilon_{\mathbf{p}} - \varepsilon_{\mathbf{p}+\mathbf{k}} + i/\tau_m)(\varepsilon_{\mathbf{p}+\mathbf{k}} - \varepsilon_{\mathbf{p}} - i/\tau_m)},$$

where $f(\varepsilon_{\mathbf{k}})$ denotes the Fermi function of energy $\varepsilon_{\mathbf{k}}$. Fig. (4) shows the resulting dynamical conductivity as a function of frequency ω for various temperatures. By expanding $M(z)$ at low temperatures in powers of ω and $\exp(-\Delta/T)$, we obtain the standard Drude Lorentzian form [23]: $\sigma(\omega) = \alpha(\omega_p^2/4\pi)(i\omega + \tau_{\text{tr}}^{-1})/(\omega^2 + \tau_{\text{tr}}^{-2})$, where $\alpha = (1 + \partial M'/\partial \omega|_{\omega=0})^{-1}$ and $\tau_{\text{tr}} = 1/\alpha M''(0)$ is the transport relaxation time. The dc resistivity is related to the transport lifetime as $\rho(T) = (4\pi/\alpha \omega_p^2) \tau_{\text{tr}}^{-1}(T)$. Fig. 5(a) shows the dc resistivity $\rho(T)$ vs temperature for various dimensionless parameter $\eta = \varepsilon_F \tau_{m,0}$. Similar to the electronic relaxation time, the resistivity increases to a maximum value as T tends to zero. At low temperatures we again find that $\rho(T)$ decreases exponentially with T :

$$\rho(T) = \rho_0 \left(1 - \frac{8}{3\pi} \frac{p_F}{\Lambda} \frac{e^{-\Delta/T}}{\varepsilon_F \tau_{m,0}} + \dots \right), \quad (9)$$

where $\rho_0 \propto (g^2/K)(\rho_F^2 \varepsilon_F / n_e \omega_p^2)$ is the residual resistivity at zero temperature.

To leading linear approximation, we use the Matthiessen's rule to combine various contributions to the resistivity. In particular, we consider a temperature dependence: $\rho_{\text{tot}}(T) \sim \rho_0 - \mathcal{A} e^{-\Delta/T} + \mathcal{B} T^n$, where \mathcal{A} is the coefficient of the exponential term in (9) and $\mathcal{B} > 0$. For example, the exponent $n = 2$ for scattering due to electron-electron interaction in a Fermi liquid. We find

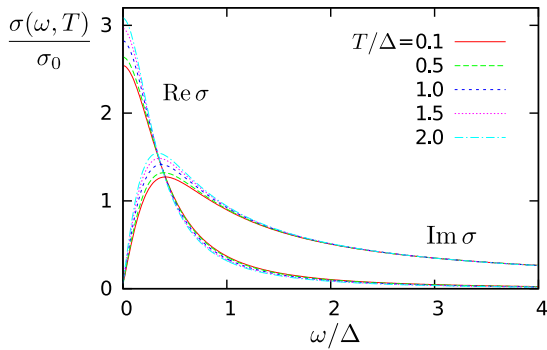


FIG. 4: (Color online) Dynamical conductivity $\sigma(\omega, T)$ as a function of frequency ω at various temperatures. The conductivity is measured with respect to $\sigma_0 = \omega_p^2/4\pi\Delta$.

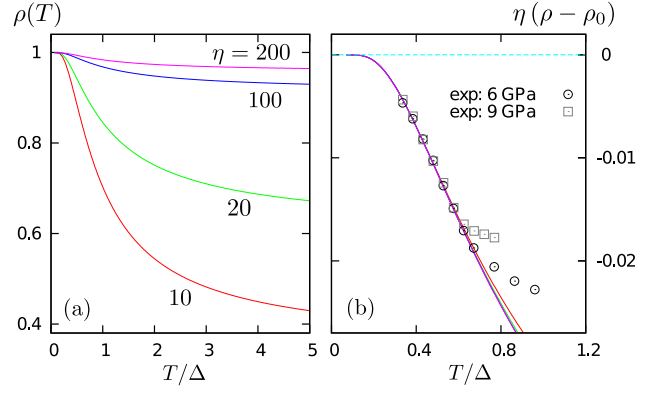


FIG. 5: (Color online) (a) Resistivity $\rho(T)$ (in units of ρ_0) as a function of temperature T for varying dimensionless parameter $\eta = \varepsilon_F \tau_{m,0}$. The Fermi energy is fixed at $\varepsilon_F = 100\Delta$ in the calculation. (b) The rescaled resistivity $\eta(\rho - \rho_0)$ collapses on a universal curve at low temperatures. Also shown is the rescaled experimental data from the measurements on $\text{Nd}_2\text{Ir}_2\text{O}_7$ [15].

that the resistivity has a minimum at

$$T_{\text{min}} = \frac{\Delta/(n+1)}{\left| W\left(\frac{-\Delta}{n+1} \left(\frac{\mathcal{B}n}{\mathcal{A}\Delta} \right)^{\frac{1}{n+1}} \right) \right|}, \quad (10)$$

for $\mathcal{A} > \mathcal{A}_c = n\mathcal{B}/\Delta (\Delta/(n+1)e)^{n+1}$. Here $W(x)$ denotes the Lambert W -function. Since $-1 < W(-x) < 0$ for $x > 0$, the resistivity minimum thus occurs at temperature scales associated with the magnetic monopole excitation energy, consistent with the numerical calculation in Ref. [17].

Experimentally, the resistivity upturn observed in $\text{Nd}_2\text{Ir}_2\text{O}_7$ under pressure agrees well with our calculations. Eq. (9) shows that the low- T resistivity curves $\eta(\rho - \rho_0)$ rescaled by the dimensionless parameter $\eta = \varepsilon_F \tau_{m,0}$ collapse on a universal curve independent of the magnetic relaxation time. By plotting the rescaled experimental resistance $R_{\text{exp}} - R_0$ as a function of T/Δ , the data points indeed fall on the theoretical curve at low temperatures [Fig. 5(b)]. From this analysis, we obtain a monopole activation energy $\Delta \approx 5.2$ K, independent of applied pressures, and a residual resistance $R_0 \approx 0.87 \Omega$ and 0.52Ω for samples under pressure 6 and 9 GPa, respectively. The ratio of the dimensionless parameters $\eta(P)$ at the two pressure values P is $\eta(6 \text{ GPa})/\eta(9 \text{ GPa}) = 3$, i.e. the prefactor of the magnetic relaxation rate $1/\tau_{m,0}$ increases by a factor of three as the pressure is increased from 6 to 9 GPa. This is not unexpected, since the spin-spin separation shrinks under pressure and, consequently, the exchange coupling increases. We also note that, while the resistivity minimum observed in the other compound $\text{Pr}_2\text{Ir}_2\text{O}_7$ is compatible with our model prediction, the low temperature data seems to suggest a $\ln T$ behavior [14], implying the effect of partial Kondo-screening.

In summary, we have shown that electronic transport in spin ice exhibits a resistivity minimum that does not originate from Kondo screening. Instead, it comes from the scattering of electrons by a random magnetization field with long-range correlation, which is controlled by thermally excited topological defects, or emergent magnetic monopoles. Using the memory function approach, we have shown that the dc resistivity decreases with increasing temperatures, in agreement with experiment and with numerical simulations of the Kondo-lattice model. Our theory opens a new route to explore unusual transport phenomena in metallic geometrically frustrated magnets. Questions that remain open, and deserve further study, are how the magnetic relaxation rate is affected by quantum spin dynamics and the feedback effect of the itinerant electrons on the local moments correlations.

Acknowledgement. We gratefully acknowledge insightful discussions with C. D. Batista, A. V. Chubukov, A. Kamenev, I. Martin, R. Moessner, Y. Motome, and M. Udagawa. G.W.C. thanks the support of the LANL Oppenheimer Fellowship.

-
- [1] J. Kondo, Prog. Theor. Phys. **32**, 37 (1964).
 - [2] S. Doniach, Physica B **91**, 231 (1977).
 - [3] A. C. Hewson, *The Kondo Problem to Heavy Fermions* (Cambridge University Press, 1993).
 - [4] S. Jin, T. H. Tiefel, M. McCormack, R. A. Fastnacht, R. Ramesh, and L. H. Chen, Science **264**, 413 (1994).
 - [5] N. Nagaosa, J. Sinova, S. Onoda, A. H. MacDonald, N. P. Ong, Rev. Mod. Phys. **82**, 1539 (2010).
 - [6] C. Zener, Phys. Rev. **82**, 403 (1951).
 - [7] Y. Machida, S. Nakatsuji, S. Onoda, T. Tayama, and T. Sakakibara, Nature **463**, 210 (2010).
 - [8] L. Balicas, S. Nakatsuji, Y. Machida, and S. Onoda, Phys. Rev. Lett. **106**, 217204 (2011).
 - [9] S. T. Bramwell and M. J. P. Gingras, Science **294**, 1495 (2001).
 - [10] A. Ikeda and H. Kawamura, J. Phys. Soc. Jpn. **77**, 073707 (2008).
 - [11] C. L. Henley, Annu. Rev. Condens. Matter Phys. **1**, 179 (2010).
 - [12] I. A. Ryzhkin, J. Exp. Theor. Phys. **101**, 481 (2005).
 - [13] C. Castelnovo, R. Moessner, and S. L. Sondhi, Nature **451**, 42 (2008).
 - [14] S. Nakatsuji, Y. Machida, Y. Maeno, T. Tayama, T. Sakakibara, J. van Duijn, L. Balicas, J. N. Millican, R. T. Macaluso, and J. Y. Chan, Phys. Rev. Lett. **96**, 087204 (2006).
 - [15] M. Sakata, T. Kagayama, K. Shimizu, K. Matsuhira, S. Takagi, M. Wakeshima, Y. Hinatsu, Phys. Rev. B **83**, 041102 (2011).
 - [16] S. Onoda and Y. Tanaka, Phys. Rev. Lett. **105**, 047201 (2010); Phys. Rev. B **83**, 094411 (2011).
 - [17] M. Udagawa, H. Ishizuka, Y. Motome, Phys. Rev. Lett. **108**, 066406 (2012).
 - [18] L. Pauling, J. Am. Chem. Soc. **57**, 2680 (1935).
 - [19] C. Castelnovo, R. Moessner, S. L. Sondhi, Annu. Rev. Condens. Matter Phys. **3**, 35 (2012).
 - [20] L. D. C. Jaubert and P. C. W. Holdsworth, Nature Phys. **5**, 258 (2009).
 - [21] P. H. Conlon and J. T. Chalker, Phys. Rev. Lett. **102**, 237206 (2009).
 - [22] W. Götze and P. Wölfle, Phys. Rev. B **6**, 1226 (1972).
 - [23] D. Pines and P. Nozières, *The theory of Quantum Liquids* (Benjamin, New York, 1966).